FireSight: Utilizing Deep Learning for Wildfire Prediction And Determining Escape Routes

This is a non-peer reviewed preprint submitted to EarthArXiv.

Aniket Mittal (aniketmittal2624@gmail.com)
Leland High School, San Jose, CA

***Abstract* – Since 2000, seven million acres have burned every year. Yet, since robust analytics are scarce, capitalizing on machine learning algorithms have the capability to bridge gaps in decision making and effective deployment. Despite this, a major limitation in current research is resolution and accuracy. Utilizing public data from NASA's MODIS, LP DAAC, University of Idaho, and UC Irvine, 12 input features and 18,545 samples, the fire mask at day t+1 is predicted. Compared to existing datasets (FRY, FireAtlas, UCI Forest Fires, US Wildfires Catalog, Globfire and European Forest Fire Information System), this dataset contains the most variables at 1 km. resolution with the most input features. By treating the fire mask as binary and probability maps, regression and classification were performed. Several novel architectures were tested (ResNet, EfficientNet, RegNet and VGG19). A dataset scaling algorithm helped improve resolution by predicting data from existing points. The most optimal models were ResNet and Efficient Net, achieving a binary accuracy of 96.58%, precision of 72.37% and mean absolute error of 0.036. Compared to current studies, this study is around 38% more precise with 0.0142 lower mean absolute error, a significant improvement. Implementation regarding spread was implemented in two ways. With classification data and substituting resulting fire masks for previous ones, the spread of a wildfire could be mapped for various days. Additionally, with population density data and this spread, escape routes were also predicted.**

Index Terms – Wildfire Prediction, Deep Learning, Remote Sensing, Escape Routes, Dataset Augmentation

I. Introduction

Over the last few decades, wildfires have become increasingly prominent, mainly as a result of human activities, ecological and climate changes [23] [30]. That number is only projected to grow, mainly as a result of increased population growth and involvement [30]. Since 2000, an annual average of 70,072 fires has burned approximately 7.0 million acres yearly, more than double the annual amount burned in the 1990s [25]. Notable examples include the 2009 Victorian bush fires in Australia, the 2017 Portugal bush fires, and the 2018 Camp Fire in California [23]. Wildfires directly affect the human and ecological environments by destroying homes, wildlife habitat, disrupting transportation, emitting greenhouse gases, cutting power, water and gas services and hurting people and wildlife across the globe [42] [46].

Between 1998-2017, more than 6.4 million people have directly been impacted by wildfires [46]. Buildings flagged with "high" or "extreme" risks totaled 924,623 and 775,654, an estimated value of $313 billion and $220 billion, respectively [27]. They can also greatly impact wildlife and ecological diversity. Specifically, the gases released during wildfires can lead to respiratory distress, neurological impairment, oxidative stress, immunosuppression and influence wildlife behavior [33] while serving as catalysts for diseases [4]. The gases emitted are also estimated to contribute to 10% of carbon emissions per year worldwide [45].

As a result, there is a great need for wildfire prediction models optimized with deep learning [10] [40] [41]. While robust analytics are scarce, capitalizing on machine learning algorithms and automated resource tracking can help bridge gaps in decision making [40]. Effective wildfire response, specifically regarding firefighter safety and deployment of resources, is critical for reducing the size of frequent wildfires [40] [47] and are essential to "minimize the bad days" in wildfire response [47]. However, wildfire detection is very complex and a computational and ecological challenge, mainly due to the variability and various factors involved [32]. While current literature has made progress regarding resolution and accuracy (1 km), a major limitation is the pixelated resolution and relatively low accuracy with current deep-learning implementation from this particular dataset [26].

This problem is exactly what this paper seeks to tackle by enlarging visibility with data augmentation and expansion techniques and improving the performance of the convolutional neural network (CNN) by comparing a series of various pre-trained models, previously not done before on this dataset.

II. Data

In total, the dataset consisted of 18,545 samples of wildfires all across the world. The dataset provides 12 input features at 64 km. x 64 km. resolution and 1 output feature also at 64 km. x 64 km. resolution. The dataset is publicly available from [26] and was individually aggregated from public datasets on Google Earth Engine.

Specifically, **daily fire mask data** was provided from MOD14A1 V6, a comprehensive dataset which utilizes absolute detection of a fire to provide fire masks at 1 km.

resolution [22]. The data was taken from NASA's MODIS, a product of the Land Processes Distributed Active Archive Center (LP DAAC) [21] [43]. **Topography data** was provided from the Shuttle Radar Topography Mission (SRTM) [19] from the National Geospatial-Intelligence Agency and NASA, which provides satellite data on elevation at 30-meter resolution [31]. **Weather data** (temperature, precipitation, winds, and humidity) was aggregated from the Gridded Surface Meteorological dataset (GRIDMET) from the University of Idaho, providing 4 km. resolution data from the University of California Irvine [1]. **Drought data** was taken from the GRIDMET Drought: CONUS Drought Indices dataset [2], where the Palmer Drought Severity Index (PDSI) was extracted for the purposes of this paper. **Vegetation data** (National Difference Vegetation Index) was provided by the NASA Visible Infrared Imaging Radiometer Suite (VIIRS) Vegetation Indices of the Suomi National Polar-Orbiting Partn ership (S-NPP) [18]. Lastly, **population density** was provided by The Gridded Population of World Version 4 which provided world population distribution at high resolution [11].

For this paper, the following input features were utilized: National Difference Vegetation Index (NDVI) [44], Elevation, Energy Release Component [8], Palmer Drought Severity Index (PDSI) [15], Population, Precipitation, Specific Humidity, Wind Direction, Min/Max Temperature, Wind Speed and Previous Fire Mask (fire mask on day t). The input features were used to output Fire Mask (fire spread on day t+1).

Any numbers that weren't feasible in real life—i.e., population being negative—were removed from the dataset. Figure 1 outlines the distribution of the data with appropriate data processing.

feature name	size	min	1stQtr	2ndQtr	3rdQtr	max	mean	std
NDVI	61353984	-3826.000	3735.000	5520.000	7123.000	9282.000	5351.794	2179.282
elevation	61353984	0.000	119.000	611.000	1595.000	3536.000	896.443	842.187
erc	61353984	0.000	30.999	49.440	75.067	109.925	53.468	25.084
pdsi	61353984	-6.056	-2.609	-1.355	1.189	6.743	-0.773	2.437
population	61353984	0.000	0.000	0.166	3.538	2935.755	29.357	190.026
pr	61353984	0.000	0.000	0.000	0.000	19.242	0.319	1.439
sph	61353984	0.000	0.004	0.006	0.008	0.086	0.007	0.004
th	61353984	0.000	149.760	208.086	254.313	360.000	199.426	71.585
tmmn	61353984	253.200	277.875	283.079	287.881	299.631	282.773	7.422
tmmx	61353984	253.200	293.976	299.818	304.222	317.387	298.638	7.894
vs	61353984	0.000	2.716	3.427	4.332	9.737	3.627	1.303

Fig. 1. dataset statistics (NDVI: National Difference Vegetation Index; Elevation: m.; ERC: Energy Release Component (BTU/ft2); PDSI: Palmer Drought Severity Index; Population: persons/km2.; PR: Precipitation (mm); SPH: Specific Humidity; TH: Wind Direction (degrees clockwise from north); TMMN / TMMX: Min/Max Temperature (Kelvin); VS: wind speed (m/s)).

Figure 2 demonstrates 3 samples of data and the various input and output features:

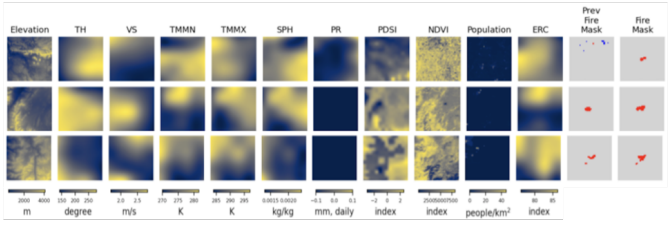

Fig. 2. three 64 km. by 64 km. samples from the training dataset. (PrevFireMask: fire mask at Day t; FireMask: fire mask at day t+1 where blue is unnamed or unclear data, red is fire, and silver is no fire).

The input features were used because they followed such criteria: were accessible with Google Earth Engine and satellite data, were available at 1 km. resolution, were publicly available and compiled from [26] and included components of the "fire-behavior triangle" (weather, topography and fuels), which are influencing factors of wildfires [20].

This dataset was chosen because it includes the most variables at 1 km resolution. Datasets like FRY [29], also collected from MODIS, FireAtlas [5], the UCI Forest Fires dataset [12] and the US Wildfires catalog [36] don't provide the input features or parameters needed for wildfire prediction but rather the sum burned area each day. Other datasets have also aggregated data from MODIS but none provide the same level of input features or with the same resolution as this one. Some examples include a study from Morocco [34], Globfire [7] and EFFIS (European Forest Fire Information System) [17].

III. Methods

A. Deep Learning Application

Deep learning was implemented with TensorFlow (https://www.tensorflow.org/) and Keras (https://keras.io). The dataset was split into training (80%, n=14,836) and testing (20%, n=3,709) data. The training set is larger dataset used to train regression models to extract pertinent features while the test set is utilized to evaluate real performance of the model against new data. Deep learning was implemented with K-Fold Cross Validation (k=5) [6], meaning the input and datasets consisted of different samples with each iteration. For cross validation, the dataset was divided into separate folds, where the test dataset alternated between the folds. The average of the output statistics was taken. This yields a more accurate assessment of the model and prevents overfitting (when a statistical model fits exactly or "memorizes" its training data). Across all models, an initial learning rate of 0.001 was utilized with a batch size of 100 and 75 epochs. We also utilized dataset augmentation techniques, extracting random 50 km. x 50 km. sections which helps introduce regularization and prevent overfitting [16]. Since pretrained models like ResNet are only fit three input channels as it is pertinent for image classification, the input layers were adjusted for the 64 km x 64 km resolution and 12 input features. A reshape layer was added to output to produce a single 64 x 64 array or the Fire Mask at day t+1. For all the models, Adam was used as the optimizer, which utilizes back propagation for stochastic gradient descent during training to enhance loss [28].

We first employed ResNet Convolutional Neural Network (CNN) architecture. To solve the degradation / vanishing gradient problem (as the gradient approaches zero, it is eliminated when reaching the deeper layers of the network), ResNet utilizes residual skip connections [24]. ResNet employs skip connections via addition, calculating the identity function of the output of the previous layer and adding it to the next, preserving the gradient [3]. The architecture was tested with the 50- and 101-layer versions, ResNet50 and ResNet101 respectively.

We then tested EfficientNet CNN architecture. EfficientNet utilizes compound scaling which uniformly scales the

network's width, depth and resolution with a set of fixed scaling coefficients in order to capture finer patterns of the input images [38]. The fixed equation for compound scaling is given by: $\alpha * \beta^2 * \gamma^2 \approx 2$ where α is depth, β is width and γ is resolution. For the EfficientNet architecture, we tested the base EfficientNet-B0 Network and the EfficientNet-V2S network, which utilizes a combination of training-aware neural network search and scaling to decrease overfitting and minimize loss, making the model more accurate but utilizing less memory [39].

Third, we tested VGG CNN architecture which utilized 16 or 19 weight layers to achieve higher depth and better performance while maintaining simplicity [37]. We tested VGG-19 which is a version of this architecture with 19 layers.

Lastly, we utilized the RegNet CNN architecture. RegNet utilizes a series of multiple stages each individually containing a series of multiple standard residual bottleneck blocks with group convolution, yielding higher accuracy and flexibility. Since RegNet is not defined by fixed parameters like other models but rather a quantized linear function that uses selected parameters, RegNet has much greater flexibility with parameter choice [35]. We tested RegNet with the X002 variant of the architecture.

B. Prediction Approaches

We utilized both classification and regression approaches in order to predict the fire mask at day $t + 1$. All architectures were tested in both approaches.

The first was binary classification. The fire mask was treated as a binary map where each 1 km $\times$ 1 km unit represented either 'fire' or 'no fire'. Binary Cross-Entropy was utilized as the loss function:

$$\mathbf{L}\left(\hat{\mathbf{y}}, \mathbf{y}\right) = -\frac{\mathbf{1}}{m}\sum_{i=1}^{m} y_i \log\left(\widehat{y}_i\right) + \left(1 - y_i\right) \log\left(\mathbf{1} - \widehat{y}_i\right)$$

To assess the performance of the binary classification model, the Receiver Operating Characteristic (ROC) curve was utilized. ROC graphically represents the true positive rate (TPR) or the proportion of correctly identified positive instances versus the false positive rate (FPR) or the proportion of incorrectly identified negative instances at various thresholds. The Area under the ROC (AUC) as well as binary accuracy were utilized to evaluate the performance of the classifier.

The second prediction approach was regression. The fire mask was treated as a probability map where each unit represented the likelihood of a fire between 0 and 1. Mean-Squared Error was utilized as the loss function:

$$\mathbf{MSE} = \frac{\mathbf{1}}{n}\sum_{i=1}^{n}\left(y_i - \widehat{y}_i\right)^2$$

To assess the performance of the model, Mean Absolute Error (MAE) is used. MAE is the average of the absolute differences between the predicted output fire mask and the actual fire mask at day $t + 1$:

$$\mathbf{MAE} = \frac{\mathbf{1}}{n}\sum_{i=1}^{n}\left|\mathbf{y}_i - \widehat{\mathbf{y}}_i\right|$$

C. Non-Deep Learning Models

For base comparison, two non-deep learning models were implemented: Logistic Regression and Random Forest.

The Logistic Regression model was implemented with TensorFlow. Adam is utilized as the optimizer with a learning rate of 0.001. To implement logistic regression, the input features are flattened into a 1D array which is fed into a Dense layer with Sigmoid activation. Binary Cross-Entropy is used as the loss function. This model was trained with 75 epochs and was tested for classification.

The Random Forest model was implemented with SciKitLearn (https://scikit-learn.org/). Random Forests utilize a series of decision trees that are trained on different subsets of the input data. By accounting for this variance, random forests reduce the risk of overfitting and bias [9]. Like the logistic regression model, the inputs and outputs were flattened and reshaped to adjust for the various features and 2D arrays. Random Forest was utilized for regression.

Like the deep learning models, the regression models were evaluated with MAE while the classification models were evaluated with Binary Accuracy and AUC.

D. Dataset Scaling Algorithm

In order to address the issues of resolution, dataset augmentation via scaling was utilized. An example of the implementation of this algorithm on a 3x3 array is displayed in Figure 3.

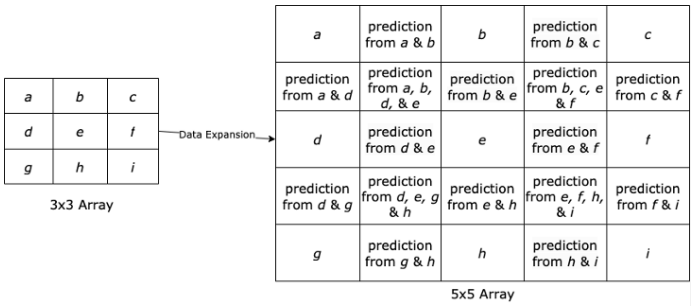

Fig. 3. the data expansion algorithm utilized for a simple 3x3 array to be converted to a 5x5 array.

The algorithm makes predictions for data points based on neighboring data points. The algorithm was utilized to convert the 64 km x 64 km features to 127 x 127 features at 0.5 km resolution as well as to 253 x 253 features at 0.25 km resolution. From these arrays, random 100 x 100 and 200 x 200 0.25-km samples were extracted. The prediction was derived from two scaling functions: average and random integer in between the neighboring values.

Two different approaches were tested. The first approach consisted of scaling the 12 input features and maintaining the 64 km x 64 km resolution of the output arrays while the second approach consisted of scaling both the input and output features. The approaches were tested to determine if scaling the input arrays yielded better performance in the model by making finer patterns between the data points.

E. Escape Route Algorithm

We present **FireSight**, an algorithm for mapping the spread of the wildfire and creating effective escape routes. By substituting the t+1 prediction as the previous fire mask, we can predict the fire masks for t+2, t+3, … Similarly, by utilizing such predictions, escape routes can be created. Utilizing population density, the center of the area of greatest population density was isolated. With this start point, the algorithm iterates through neighboring values, determining the point furthest from the fire. Figure 4 demonstrates a flowchart of the algorithm process for one iteration.

Fig. 4. Flow chart depicting one iteration of the FireSight algorithm; continues until the end of the map is reached.

Assuming that individuals can travel 4 km. in one day, the FireSight algorithm continues this process of finding the furthest neighboring values from the fire until it reaches the end of the map.

IV. Results

A. Binary Classification

By treating the fire masks as binary maps, classification was implemented. Binary Accuracy, AUC and Precision were utilized to evaluate the performance of the model.

We first tested logistic regression for comparison. Implemented with a batch size of 100 and 75 epochs—any further epochs were computationally expensive, led to further overfitting and didn't yield significant performance increases, the logistic regression model yielded a binary accuracy of 0.9179, AUC of 0.5107 and precision of 0.050.

Classification was then implemented with the deep-learning architectures. Through preliminary testing, a batch size of 100 and 75 epochs were optimal for both performance and computational cost. The models were implemented with K-Fold Cross-Validation and the average statistics were taken across all folds. The results across different architectures are illustrated in Figure 5.

Binary Classification Results:

	Training			**Testing**		
	Binary Accuracy	AUC	Precision	Binary Accuracy	AUC	Precision
ResNet50	0.9680	0.6145	0.7635	0.9648	0.5631	0.4712
Resnet101	0.9654	0.5725	0.6249	0.9642	0.5529	0.5422
EfficientNet	0.9664	0.6042	0.6687	0.9652	0.5725	0.5843
EfficientNetV2S	0.9660	0.5701	0.7001	0.9658	0.5836	0.7183
RegNetX002	0.9654	0.5669	0.6487	0.9653	0.5641	0.6357
VGG19	0.9650	0.5698	0.6859	0.9658	0.5693	0.6823

Fig. 5. Average Epochs vs. Binary Accuracy, AUC, and Precision with ResNet50, ResNet101, EfficientNet, EfficientNetV2S, RegNetX002 and VGG19 for Training and Testing Sets

With 20,837,272 parameters, EfficientNtV2S performed the best across all folds achieving a Binary Accuracy of 0.9658, an AUC of 0.5836 and a Precision of 0.7183 on the test dataset while barely overfitting as the performance on the training set was poorer than the test dataset.

B. Regression

By treating the fire masks as probability maps, regression was implemented. MAE was utilized to evaluate the performance of the models.

For comparison, a Random Forest model was tested. The model was implemented with a batch size of 50 and 10 epochs as further epochs were very computationally expensive without significantly better performance through preliminary testing. The Random Forest achieved an MAE of 0.0840.

We then implemented regression on the deep-learning architectures. Through preliminary testing, a batch size of 100 and 75 epochs were reasoned to be optimal regarding computational demand, accuracy and preventing excessive overfitting. A total of five folds were implemented for K-Fold Cross-Validation and the average was taken across all folds for MAE. The MAE loss for the training and test sets for the best-performing fold is demonstrated in Figure 6. The average MAE loss across all folds for both training and test datasets are displayed in Figure 7.

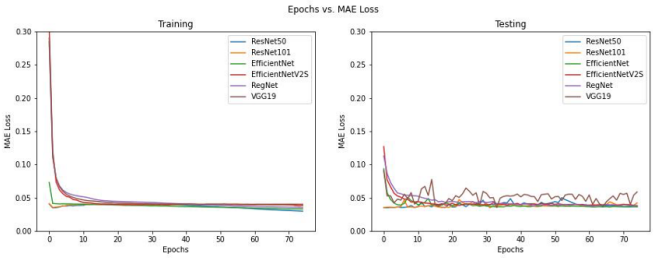

Fig. 6. Epochs vs. MAE Loss for Fold 1 with ResNet50, ResNet101, EfficientNet, EfficientNetV2S, RegNetX002 and VGG19 for Training and Testing Sets

Average MAE Loss Across All Folds

	Training	**Testing**
ResNet50	0.0292	0.0370
ResNet101	0.0339	0.0359
EfficientNet	0.0317	0.0367
EfficientNetV2S	0.0384	0.0376
RegNetX002	0.0353	0.0374
VGG19	0.0383	0.0387

Fig. 7. Average Epochs vs. MAE Loss across all folds with ResNet50, ResNet101, EfficientNet, EfficientNetV2S, RegNetX002 and VGG19 for Training and Testing Sets

With 51,079,104 parameters, ResNet101 performed the best, achieving an average testing MAE of 0.0359. However, the model can be quite computationally expensive with that many

parameters. When measuring MAE to parameter ratio, RegNetX002 performed the best with only 2,580,544 parameters and a MAE of 0.0374.

C. Dataset Scaling

We applied the dataset scaling algorithm towards improving the resolution of the model. It was utilized to extract 120x120 0.5-km regions from the current samples. Two approaches were tested: one in which only the input parameters were scaled (Approach 1) and one in which both parameters were scaled (Approach 2). The approaches were tested with different prediction equations: average where the average cross the neighboring values were taken and random where a random integer between the two values was taken.

We utilized the best performing algorithms from the results above, specifically EfficientNetV2S for classification and ResNet101 for Regression. The results are shown below in Figure 8.

Average Regression and Classification Results with Dataset Scaling

	Regression	Classification		
	MAE	Binary Accuracy	AUC	Precision
Approach 1 with Average	0.0365	0.9660	0.5730	0.7237
Approach 1 with Random	0.0415	0.9512	0.5645	0.6981
Approach 2 with Average	0.0391	0.9599	0.5704	0.7143
Approach 2 with Random	0.0401	0.9520	0.5691	0.6792

Fig. 8. Average regression and classification results across 5 folds utilizing ResNet101 (Regression) and EfficientNetV2S (Classification) with 120x120 0.5-km samples obtained with dataset scaling.

The results highlight that Approach 1 with Average performed the best since the model was able to determine finer patterns across the input features and better predict the locations of the fire maps. The model achieved a MAE of 0.0365, Binary Accuracy of 0.9660, AUC of 0.5730 and Precision of 0.7237, better than the base-models.

D. FireSight Implementation

After predicting wildfires, Fire Sight was utilized to trace the spread of a wildfire over the course of one week. The wildfire spread and escape route is illustrated in Figure 9.

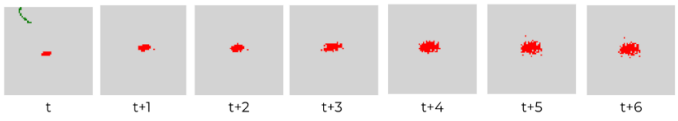

Fig. 9. example of fire spread (red) across 1 week (t=7 days) and the predicted escape route (green).

V. Discussions

From the experiment, ResNet101 and EfficientNetV2S performed the best for classification and regression, respectively. They each had low levels of overfitting with a 0.002 difference in MAE between training and testing for ResNet101 and an increase of 0.01 in AUC and 0.0182 in precision, clearly demonstrating low levels of overfitting.

Several explanations can explain the increase in performance for both EfficientNetV2S and ResNet101. A more modern approach, EfficientNetV2S utilizes compound scaling to capture finer patterns at different scales, often beneficial for classification tasks. In contrast, ResNet101 is more traditional with a large number of layers, often better suited to regression tasks which require complex feature extraction. In addition, the performance can best be explained since these architectures are computationally simple but yet deeper-level architectures with higher levels of parameters, allowing the model to notice finer patterns and make better predictions.

Compared to current literature, the model yields better accuracy with similar levels of input features. In comparison to the study by Huot [26], the model has 38.77% higher precision and 29.96% increased AUC which allows the model to make more accurate predictions. In addition, specifically for regression for wildfire spread, compared to work by Cruz [13] [14], the MAE of 0.142 lower, a significant improvement. Overall, the model both yxields better performance and is able to incorporate better resolution. In addition, contrary to previous studies, we present FireSight which is a new algorithm for predicting spread of wildfires and determining optimal escape routes based on population.

However, there are several limitations to consider in this study. First, some resulting fire maps were offset towards the center of the screen, a result of the final Dense output layer. Second, the dataset scaling algorithm that we presented doesn't actually make real data points but rather predictions from neighboring points as approximations introducing some limitations. Lastly, the wildfire spread was traced utilizing predictions and does not reflect real fire masks. Especially since the model is trained to predict the fire mask at t+1 and not the wildfire spread itself.

Future research can include adapting the GEE code to include fire maps on multiple days (t+2, t+3, t+4...) to accurately map progression rather than just a resulting fire map. The dataset scaling algorithm can also be modified to incorporate more neighboring values rather than just the ones surrounding the point to make more accurate predictions. In addition, we can utilize further dataset augmentation techniques to reduce the problems with overfitting and attain higher levels of resolution.

VI. Conclusions

Utilizing deep learning with both classification and regression, we were successfully able to predict the fire mask from the 12 input features and assess the performance with MAE, Binary Accuracy, Precision and AUC. We also present FireSight, serving as a tool to find escape routes by tracing fire map spread. Compared to current literature, the model is more accurate with greater number of input features and resolution. While further research is necessary to create a more concrete system for effective firefighter response and civilian safety, our model can serve as a better method for predicting wildfires with higher-resolution features. Future research can focus on utilizing deep learning to specifically predict spreads and incorporate more input parameters to maximize efficiency and determine relationships which contribute to wildfire spread.

VII. Funding

The author declares that no funds, grants, or other support were provided during the creation of this manuscript.

VIII. Conflict of Interest

The author declares that they have no conflict of interest in the conduction of this study.

IX. Author Contributions

A.M.: Conceptualization, methodology, data processing, machine learning implementation, algorithm development, data visualization, model performance visualization, validation, background research, paper editing

References

[1] John T Abatzoglou. Development of gridded surface meteorological data for ecological applications and modelling. *International Journal of Climatology*, 33(1):121–131, 2013.

[2] John T Abatzoglou, David E Rupp, and Philip W Mote. Seasonal climate variability and change in the pacific northwest of the united states. *Journal of Climate*, 27(5):2125–2142, 2014.

[3] Nikolas Adaloglou. Intuitive explanation of skip connections in deep learning. *AI Summer*, 2020.

[4] Gregory F Albery, Isabella Turilli, Maxwell B Joseph, Janet Foley, Celine H Frere, and Shweta Bansal. From flames to inflammation: how wildfires affect patterns of wildlife disease. *Fire Ecology*, 17(1):1–17, 2021.

[5] Niels Andela. Global fire atlas, Apr 2019.

[6] Davide Anguita, Luca Ghelardoni, Alessandro Ghio, Luca Oneto, and Sandro Ridella. The'k'in k-fold cross validation. In *ESANN*, pages 441–446, 2012.

[7] Tomàs Artés, Duarte Oom, Daniele De Rigo, Tracy Houston Durrant, Pieralberto Maianti, Giorgio Libertà, and Jesús San-Miguel-Ayanz. A global wildfire dataset for the analysis of fire regimes and fire behaviour. *Scientific data*, 6(1):296, 2019.

[8] L Beth, Brown TJ, Bradshaw LS, and Jolly WM. National standardized energy release component (erc) forecasts. In *5th Symposium on Fire and Forest Meteorology*, 2003.

[9] Leo Breiman. Random forests. *Machine learning*, 45:5–32, 2001.

[10] David R Brillinger, Haiganoush K Preisler, and John W Benoit. Risk assessment: a forest fire example. *Lecture Notes-Monograph Series*, pages 177–196, 2003.

[11] Columbia University Center for International Earth Science Information Network (CIESIN). Gridded population of the world, version 4 (gpwv4). *Population Count Adjusted to Match 2015 Revision of UN WPP Country Totals*, 2016.

[12] Paulo Cortez and Aníbal de Jesus Raimundo Morais. A data mining approach to predict forest fires using meteorological data. 2007.

[13] Miguel G Cruz, Martin E Alexander, Andrew L Sullivan, James S Gould, and Musa Kilinc. Assessing improvements in models used to operationally predict wildland fire rate of spread. *Environmental Modelling & Software*, 105:54–63, 2018.

[14] Miguel G Cruz, N Phillip Cheney, James S Gould, W Lachlan McCaw, Musa Kilinc, and Andrew L Sullivan. An empirical-based model for predicting the forward spread rate of wildfires in eucalypt forests. *International journal of wildland fire*, 31(1):81–95, 2021.

[15] Aiguo Dai. Climate data guide, Sep 2012.

[16] Tri Dao, Albert Gu, Alexander Ratner, Virginia Smith, Chris De Sa, and Christopher Ré. A kernel theory of modern data augmentation. In *International Conference on Machine Learning*, pages 1528–1537. PMLR, 2019.

[17] EFFIS Data and Services. Data and services.

[18] ABK Didan and A Barreto. Viirs/npp vegetation indices 16-day l3 global 500m sin grid v001. *NASA EOSDIS Land Processes DAAC: Oak Ridge, TN, USA*, 2018.

[19] Tom G Farr, Paul A Rosen, Edward Caro, Robert Crippen, Riley Duren, Scott Hensley, Michael Kobrick, Mimi Paller, Ernesto Rodriguez, Ladislav Roth, et al. The shuttle radar topography mission. *Reviews of geophysics*, 45(2), 2007.

[20] Mark A Finney and Patricia L Andrews. Farsite—a program for fire growth simulation. *Fire management notes*, 59(2):13–15, 1999.

[21] Shannell Frazier. Modis web.

[22] L Giglio and C Justice. Mod14a1 modis/terra thermal anomalies/fire daily l3 global 1km sin grid v006. *NASA EOSDIS Land Processes DAAC*, 2015.

[23] Katharine Haynes, Karen Short, Gavriil Xanthopoulos, Domingos Viegas, LM Ribeiro, and R Blanchi. Wildfires and wui fire fatalities. *Encyclopedia of wildfires and wildland-urban Interface (WUI) fires*, pages 1073–1088, 2020.

[24] Kaiming He, Xiangyu Zhang, Shaoqing Ren, and Jian Sun. Deep residual learning for image recognition. In *Proceedings of the IEEE conference on computer vision and pattern recognition*, pages 770–778, 2016.

[25] Katie Hoover and Laura A Hanson. Wildfire statistics. Technical report, Congressional Research Service, 2021.

[26] Fantine Huot, R Lily Hu, Nita Goyal, Tharun Sankar, Matthias Ihme, and Yi-Fan Chen. Next day wildfire spread: A machine learning dataset to predict wildfire spreading from remote-sensing data. *IEEE Transactions on Geoscience and Remote Sensing*, 60:1–13, 2022.

[27] Tom Jeffery, S Yerkes, D Moore, F Calgiano, R Turakhia, and Corelogic. 2019 wildfire risk report. *Technical Report*, 2019.

[28] Diederik P Kingma and Jimmy Ba. Adam: A method for stochastic optimization. *arXiv preprint arXiv:1412.6980*, 2014.

[29] Pierre Laurent, Florent Mouillot, Chao Yue, Philippe Ciais, M Vanesa Moreno, and Joana MP Nogueira. Fry, a global database of fire patch functional traits derived from space-borne burned area products. *Scientific data*, 5(1):1–12, 2018.

[30] Jennifer R Marlon, Patrick J Bartlein, Daniel G Gavin, Colin J Long, R Scott Anderson, Christy E Briles, Kendrick J Brown, Daniele Colombaroli, Douglas J Hallett, Mitchell J Power, et al. Long-term perspective on wildfires in the western usa. *Proceedings of the National Academy of Sciences*, 109(9):E535–E543, 2012.

[31] NASA. Shuttle radar topography mission.

[32] Carol Potera. Climate change: challenges of predicting wildfire activity, 2009.

[33] OV Sanderfoot, SB Bassing, JL Brusa, RL Emmet, SJ Gillman, K Swift, and B Gardner. A review of the effects of wildfire smoke on the health and behavior of wildlife. *Environmental Research Letters*, 16(12):123003, 2022.

[34] Younes Oulad Sayad, Hajar Mousannif, and Hassan Al Moatassime. Predictive modeling of wildfires: A new dataset and machine learning approach. *Fire safety journal*, 104:130–146, 2019.

[35] Nick Schneider, Florian Piewak, Christoph Stiller, and Uwe Franke. Regnet: Multimodal sensor registration using deep neural networks. In *2017 IEEE intelligent vehicles symposium (IV)*, pages 1803–1810. IEEE, 2017.

[36] Karen C Short. Spatial wildfire occurrence data for the united states, 1992–2015 [fpa fod 20170508]. forest service research data archive (fort collins, co, usa, 2017).

[37] Karen Simonyan and Andrew Zisserman. Very deep convolutional networks for large-scale image recognition. *arXiv preprint arXiv:1409.1556*, 2014.

[38] Mingxing Tan and Quoc Le. Efficientnet: Rethinking model scaling for convolutional neural networks. In *International conference on machine learning*, pages 6105–6114. PMLR, 2019.

[39] Mingxing Tan and Quoc Le. Efficientnetv2: Smaller models and faster training. In *International conference on machine learning*, pages 10096–10106. PMLR, 2021.

[40] Steve W Taylor, Douglas G Woolford, CB Dean, and David L Martell. Wildfire prediction to inform fire management: statistical science challenges. 2013.

[41] Matthew P Thompson, Yu Wei, David E Calkin, Christopher D O'Connor, Christopher J Dunn, Nathaniel M Anderson, and John S Hogland. Risk management and analytics in wildfire response. *Current Forestry Reports*, 5:226–239, 2019.

[42] USFS. Fire effects on the environment, 2020.

[43] USGS. Lp daac - modis overview - usgs.

[44] USGS. Landsat normalized difference vegetation index, 2018.

[45] Guido R Van Der Werf, James T Randerson, Louis Giglio, Thijs T Van Leeuwen, Yang Chen, Brendan M Rogers, Mingquan Mu, Margreet JE Van Marle, Douglas C Morton, G James Collatz, et al. Global fire emissions estimates during 1997–2016. *Earth System Science Data*, 9(2):697–720, 2017.

[46] WHO. Wildfires, 2018.

[47] Katherine Wollstein, Casey O'Connor, Jacob Gear, and Rod Hoagland. Minimize the bad days: Wildland fire response and suppression success. *Rangelands*, 44(3):187–193, 2022.